JMEPEG (2016) 25:4735–4740
DOI: 10.1007/s11665-016-2324-9

1059-9495/$19.00

Microstructure and Corrosion Resistance of Electrodeposited Ni-Cu-Mo Alloy Coatings

Xinjing Meng, Xi Shi, Qingdong Zhong, Mingyong Shu, and Guanquan Xu

(Submitted October 15, 2015; in revised form July 29, 2016; published online September 23, 2016)

This paper deals with the electrodeposition of Ni-Cu-Mo ternary alloy coatings on low-carbon steel substrate from an aqueous citrate sulfate bath. The structures and microstructure of coatings were characterized by scanning electron microscopy and x-ray diffractometry. The corrosion resistance of coatings was investigated by potentiodynamic polarization (Tafel) and electrochemical impedance spectroscopy techniques. The results show that the Ni-Cu-Mo coatings are mainly composed of fcc-Ni phase and a small amount of NiCu phase. Ni-Cu-Mo coatings exhibit a nodular surface morphology, and the roughness of electroplated coating increases with the increasing of $Na_2MoO_4{\cdot}2H_2O$ in the bath. The corrosion performance of the coatings is significantly affected by the Mo content of the alloy coating and their surface morphology. The coating prepared in bath containing 40 g/L $Na_2MoO_4{\cdot}2H_2O$ has the highest corrosion resistance in 3.5 wt.% NaCl solution, while that prepared in bath containing 60 g/L (or more) $Na_2MoO_4{\cdot}2H_2O$ shows a lower corrosion resistance due to the presence of microcracks on the coating surface.

Keywords coating, corrosion resistance, EIS, electrodeposition, Ni-Cu-Mo alloy

1. Introduction

Electrodeposition technique is widely used in industrial applications because many electroplating coatings can meet high and specific excellent performance demands (Ref 1-3). Related to their good corrosion resistances, mechanical properties and graceful appearance, Ni-Cu alloys have been widely employed for protecting metal surfaces (Ref 4, 5). So far, electrodeposition of Ni-Cu alloy coatings from aqueous plating electrolytes has been extensively investigated (Ref 6, 7), and it was found that the phase composition and morphology of Ni-Cu alloy coatings can be controlled by changing different parameters in electrodeposition process, which results in different mechanical, physical and chemical properties.

The properties of alloys can be tailored using different combinations of metals and compounds (Ref 8). For this reason, another important method to improve the properties of electrodeposits is co-deposit ternary and quaternary alloy coatings. There is extensive literatures concerning the Ni-Cu based alloy coatings, such as Ni-Cu-Fe (Ref 9), Ni-Cu-P (Ref 10, 11), Ni-Cu-Zn (Ref 12) and Ni-Cu-Mo (Ref 13-15). Among these alloying elements in Ni-Cu-based alloy as mentioned above, Mo (also a group VI metal) is expected to have similar chemical and electrochemical properties as chromium (Ref 16-18). In fact, Mo alloy is considered as a desirable new surface coating to replace hard chromium coatings, because of the environmental and toxicological restrictions on hard chromium industrial electroplating.

There are limited prior works in the literature regarding electrodeposition of Ni-Cu-Mo ternary alloy coatings except for the results presented by Beltowska-Lehman et al. (Ref 13-15).Their studies illustrate that Ni-Cu-Mo alloy could be electrodeposited at room temperature from citrate ammonia electrolytes, and its x-ray diffraction patterns exhibited a fcc structure of Ni-Cu solid solutions (Ref 13). Nickel induces molybdenum deposition but its discharge is markedly inhibited by molybdenum, and the electrocrystallization process is dominated by the Ni-Mo co-discharge kinetics (Ref 14). Copper deposition has a depolarizing effect on Ni-Mo discharge. Specially, the changes in the values of the limiting currents of Cu occurring in the presence of nickel ions are associated with the formation of a inert heteronuclear complex $[CuNi(cit)_2]^{4-}$ when the pH values are in the range from 6 to 8 (Ref 15).

However, study of the corrosion resistance of electrodeposited Ni-Cu-Mo alloy coating is rarely reported in the literature. In this paper, Ni-Cu-Mo ternary alloy coatings were prepared on mild steel substrate by the electrodeposition in citrate sulfate solution, and their corrosion resistances were investigated using the potentiodynamic polarization curves and electrochemical impedance spectroscopy (EIS) techniques in conjunction with impedance fitting.

2. Experimental

Ni-Cu-Mo alloys were electrodeposited by a direct current deposition electroplating method with the composition of the bath as shown in Table 1. The pH was adjusted to 9 by adding

Xinjing Meng, State Key Laboratory of Advanced Special Steels, School of Materials Science and Engineering, Shanghai University, Shanghai 200072, China; and Shanghai University of Electric Power, Shanghai Engineering Research Center of Energy-Saving in Heat Exchange Systems, Shanghai 200090, China; **Xi Shi, Qingdong Zhong,** and **Mingyong Shu**, State Key Laboratory of Advanced Special Steels, School of Materials Science and Engineering, Shanghai University, Shanghai 200072, China; and **Guanquan Xu**, Shanghai University of Electric Power, Shanghai Engineering Research Center of Energy-Saving in Heat Exchange Systems, Shanghai 200090, China. Contact e-mails: mengxinjing@shiep.edu.cn and xjmengtg@sina.com.

Table 1 Composition of the bath used for Ni-Cu-Mo coatings

Deposition parameters	Amount	Purpose
$NiSO_4{\cdot}6H_2O$	131.5 g/L	Ni source
$CuSO_4{\cdot}5H_2O$	1.25 g/L	Cu source
$Na_2MoO_4\cdot 2H_2O$	0, 20, 40, 60, 80 g/L	Mo source
$Na_3C_6H_5O_7{\cdot}2H_2O$	36.75 g/L	Complexer for Ni and Mo
$NiCl_2{\cdot}6\ H_20$	11.9 g/L	Increase current efficiency
$C_6H_{15}NO_3$	14.75 mL/L	Additive-A
$C_2H_5NO_2$	3.71 g/L	Additive-B

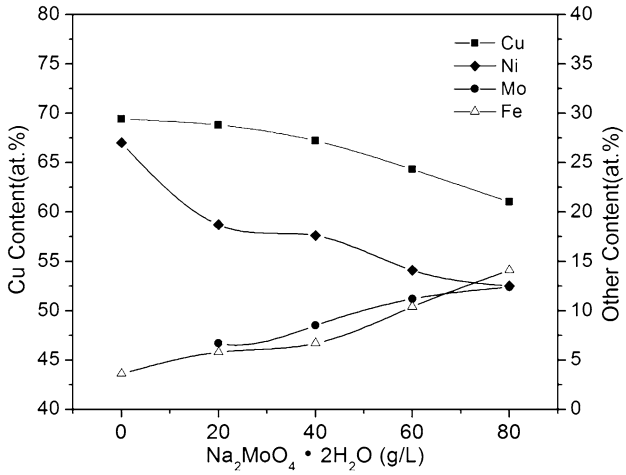

Fig. 1 Variation of composition of the coatings electroplated in the bath containing different $Na_2MoO_4{\cdot}2H_2O$

sulphuric acid. Low-carbon steel, with a 1 cm^2 area, served as the working electrode; a platinum plate was used as the anode. Both electrodes were kept in a vertical position and the solution was not agitated. The low-carbon steel cathodes were mechanically polished with different grade emery papers up to #2000 and then ultrasonically cleaned in acetone, rinsed in distilled water and activated for 10 seconds in an HCl solution (1:1) prior to electrodeposition. The deposition was carried out under galvanostatic conditions at a current density of 20 mA/cm^2. After deposition, the coatings were washed in distilled water, and then dehumidified.

After deposition, the structural characters of the coatings were investigated by x-ray diffraction (XRD) with a Bruker's D8 Advance, equipped with a primary beam monochromator for Cu-K radiation. The surface morphology of Ni-Cu-Mo coating was evaluated by scanning electron microscope (SEM) using CARL ZESS-CSM700 microscope, and the chemical composition of the coatings was determined by an Oxford Aztec HKL standard energy dispersive spectroscopy (EDX).

The corrosion behavior of electroplated Ni-Cu-Mo alloys had been evaluated by means of non-destructive electrochemical impedance spectroscopy (EIS) and destructive potentiodynamic polarization test in 3.5% NaCl solution. The measurements were made using an electrochemistry station (CHI660C), which was connected to a conventional three-electrode cell. A saturated calomel reference electrode (SCE) and a platinum mesh as counter-electrode were used in the tests. The impedance data were carried out potentiostatically at open-circuit potential, with voltage perturbation amplitude of 5 mV in the frequency range from 100 kHz to 10 mHz. Polarization curves were recorded by sweeping the electrode potential from −700 V to −300 mV at a scan rate of 1 mV/s.

3. Results and Discussion

3.1 EDX Analysis

The chemical compositions of electroplated Ni-Cu and Ni-Cu-Mo alloys were analyzed using EDX analysis and the results are shown in Fig. 1. EDX is not accurate enough in detection of light elements such as C and O (Ref 8, 19). Thus, it is assumed that the coatings are only composed of Ni, Cu and Mo in this paper although the presence of C and O element in the coating is quite probable. It reveals that the amount of Mo content in the coating alloy is dependent on the relative concentration of $Na_2MoO_4{\cdot}2H_2O$ in the electroplating bath, while Cu content decreases on the surface coating with increasing amount of $Na_2MoO_4{\cdot}2H_2O$ in the electroplating bath. It was reported that the induced co-deposition of Mo with Ni occurs with the help of a surface-adsorbed intermediate $[Ni(II)LMoO_2]ads$, where L is a ligand such as citrate (Ref 20, 21). In the current study, these surface-adsorbed intermediates on the cathode surface may be the main reason for the limited Cu deposition during the co-deposition of Mo with Ni. Moreover, little Fe element is detected due to the uncovered carbon steel on the margin or cracks.

3.2 Morphological Analysis

Figure 2 shows the morphology of Ni-Cu and Ni-Cu-Mo alloys electroplated in the bath containing different amount of $Na_2MoO_4{\cdot}2H_2O$. The morphology of the Ni-Cu coating shows a relatively smooth surface with fine grain boundaries, while the Ni-Cu-Mo coatings exhibit rough, regular, and nodular morphology. The crevices between nodulations enlarge with increasing the amount of $Na_2MoO_4{\cdot}2H_2O$ in the electroplating bath. When the amount of $Na_2MoO_4{\cdot}2H_2O$ added was more than 40 g/L, microcracks were found on the surface of Ni-Cu-Mo coatings. Generally, cracks often result from high residual stress or hydrogen embrittlement during electroplating, which are undesirable for corrosion performance (Ref 18). The surface roughness (Ra, arithmetical mean deviation of the assessed profile) of coatings is also a very important parameter to reflect surface morphology in macro-scale. As shown in Fig. 3, all Ni-Cu-Mo coatings exhibit a much bigger roughness value than that of Ni-Cu coating (only 0.099 μm), and the roughness of Ni-Cu-Mo coatings increases from 0.35 to 0.73 μm as the concentration of $Na_2MoO_4{\cdot}2H_2O$ increases. Possible reasons for this result are tendency of enlarged crevices between nodulations and appearance of microcracks when the $Na_2MoO_4{\cdot}2H_2O$ concentration increased (as shown in Fig. 2).

3.3 XRD Analysis

Figure 4 shows the XRD patterns of Ni-Cu and Ni-Cu-Mo coatings. From the obtained patterns, the reflections from one weak characteristic crystal plane of (200) for Fe are observed for all coatings. This reflection is viewed for the uncovered

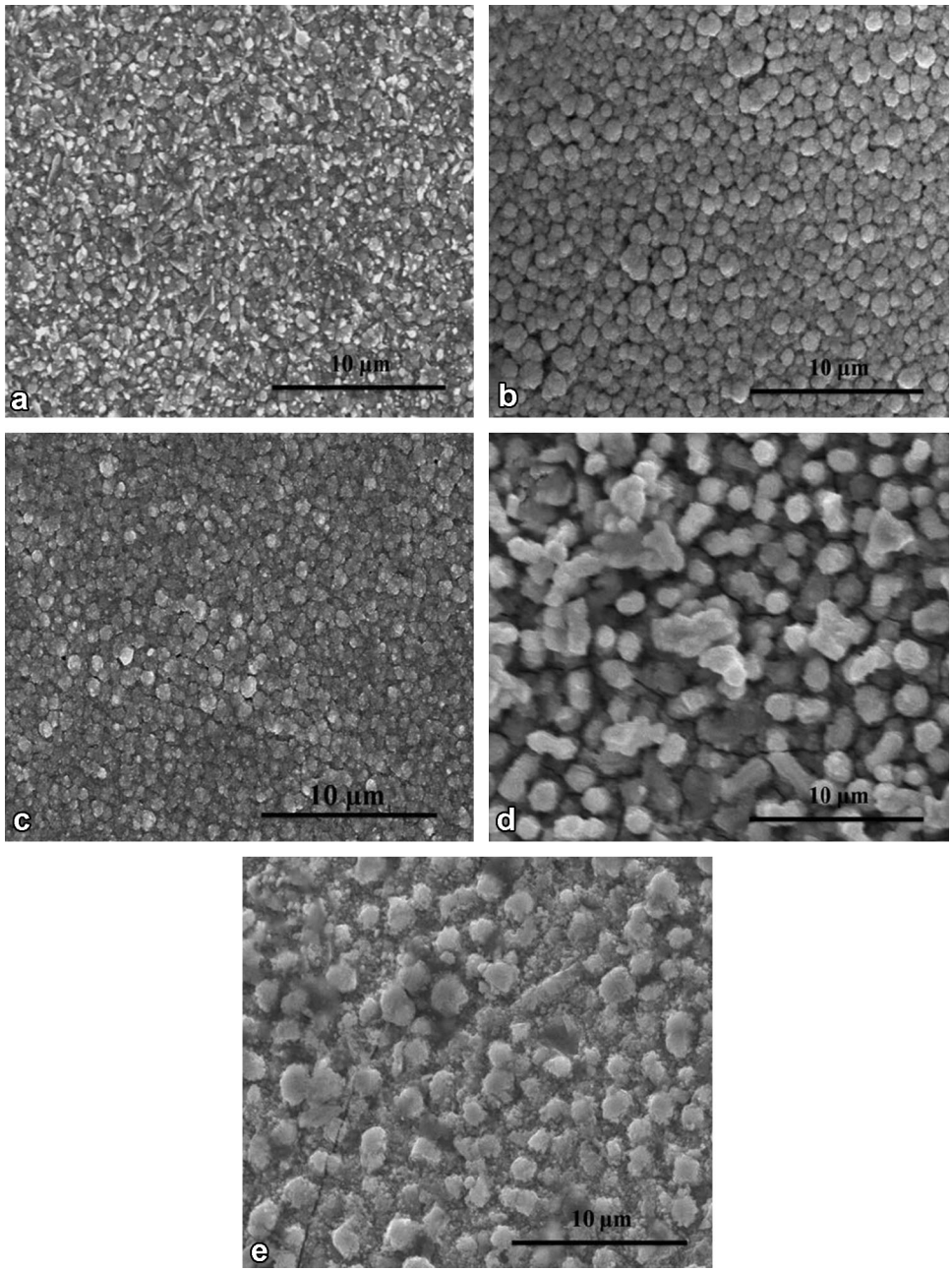

Fig. 2 Morphology of Ni-Cu and Ni-Cu-Mo alloys electroplated in the bath containing different $Na_2MoO_4{\cdot}2H_2O$: (a) 0 g/L, (b) 20 g/L, (c) 40 g/L, (d) 60 g/L, (e) 80 g/L

low-carbon steel substrate, which is in the margins or microcracks. Besides, Ni-Cu coating exhibits diffraction peaks of NiCu phase, while Ni-Cu-Mo alloy shows diffraction peaks of both NiCu phase and fcc-Ni phase. There is a sharp decrease in the intensity of NiCu phases in the Ni-Cu-Mo alloys in comparison with Ni-Cu coating, suggesting the Ni-Cu-Mo alloys were mainly constituted by Ni-fcc structure with Cu or Mo in solid solution in a Ni matrix. Taking into account the fact that Mo cannot be deposited either separately or with copper and only iron group metals can induce its discharge, it can be concluded that the electrodeposition of Ni-Cu-Mo alloy includes two different co-deposition processes: the deposition of NiCu and the induced deposition of Mo (or Cu) in a Ni matrix. Although there is a higher deposition rate of the Cu^{2+} ions due to their kinetic driving force, NiCu deposition is suppressed and fcc-Ni is deposited because the cathode surface was adsorbed by intermediates ([Ni(II)L-MoO_2]) during the formation of Ni-Cu-Mo coating. As a result, unlike the fine grain Ni-Cu coating, Ni-Cu-Mo coatings exhibited a nodular surface morphology and the Cu content decreased when the $Na_2MoO_4{\cdot}2H_2O$ was added in the electroplating bath. These results are fairly consistent with the above results drawn out of the SEM micrographs and EDX analysis. These results are fairly consistent with the above results drawn out of the SEM micrographs and EDX analysis, as shown in Fig. 1 and 2.

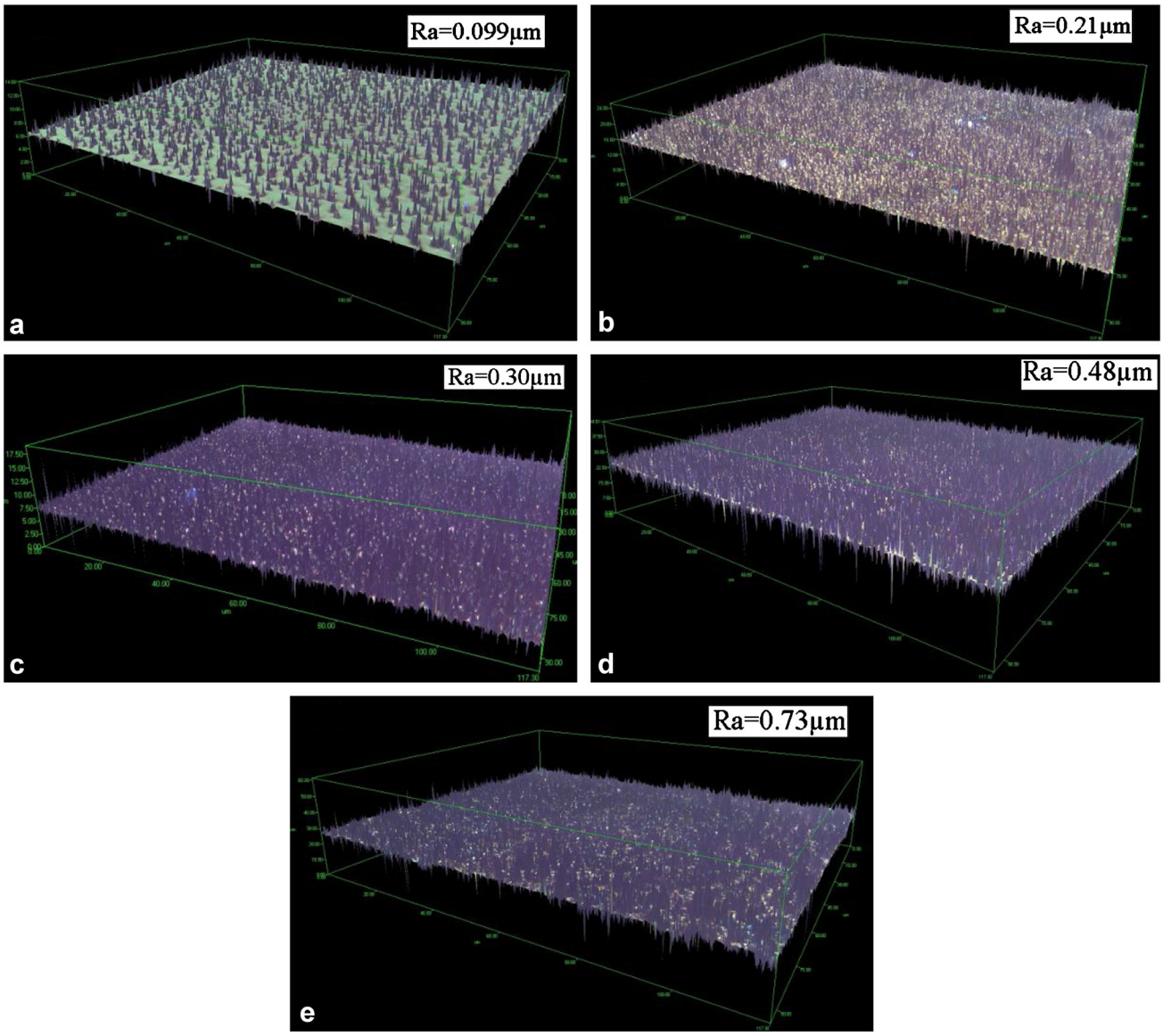

Fig. 3 The roughness of Ni-Cu and Ni-Cu-Mo alloys electroplated in the bath containing different $Na_2MoO_4{\cdot}2H_2O$: (a) 0 g/L, (b) 20 g/L, (c) 40 g/L, (d) 60 g/L, (e) 80 g/L

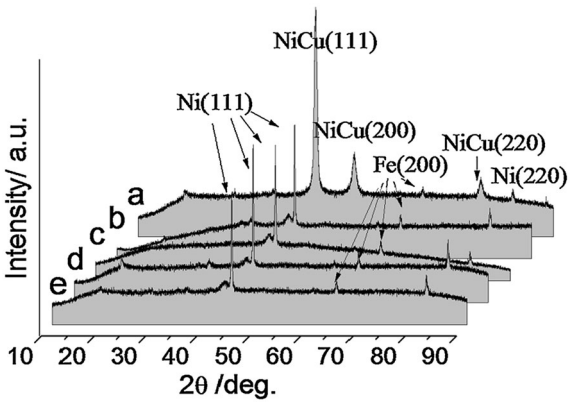

Fig. 4 X-ray diffraction patterns of Ni-Cu and Ni-Cu-Mo alloys electroplated in the bath containing different $Na_2MoO_4{\cdot}2H_2O$: (a) 0 g/L, (b) 20 g/L, (c) 40 g/L, (d) 60 g/L, (e) 80 g/L

3.4 Evaluation of Corrosion Performance

Figure 5 shows the Tafel plots (E versus log i) of Ni-Cu and Ni-Cu-Mo alloys in 3.5 wt.% NaCl solution. The related parameters extracted from the plots using Tafel extrapolation method are listed in Table 2. As it is seen from Fig. 5 and Table 2, all Ni-Cu-Mo coatings have more positive corrosion potential than those of Ni-Cu coatings, for which a more excellent corrosion resistance property is expected. Besides, a highest corrosion resistance (lowest corrosion current density) is obtained for the coatings deposited in the bath containing 40 g/L $Na_2MoO_4{\cdot}2H_2O$. As mentioned above, the Mo content in the alloy coating has a beneficial effect on the corrosion behavior. However, the corrosion current density of coatings deposited in baths containing 60-80 g/L $Na_2MoO_4{\cdot}2H_2O$ increases though the corrosion potential of them remains toward positive, as listed in Table 2. Morphological analysis has revealed that microcrack appeared on the surface of these two samples, which imply that the corrosive medium could

penetrate into the cracks, transfer through the coatings and reach the substrate. Finally, corrosive medium can react with the low-carbon steel substrate, which results in increasing corrosion current density.

Electrochemical impedance spectroscopy (EIS) is a non-destructive electrochemical technique to affirm corrosion behaviors at the electrode/electrolyte interface (Ref 22). Its result is usually displayed either in the form of a Bode plot or a Nyquist plot. The Nyquist plots of most coatings show a similar circle arc, which relates to changes in the coating property, as shown in Fig. 6. Specially, Nyquist plots of coatings deposited in baths containing 60-80 g/L $Na_2MoO_4{\cdot}2H_2O$ have an other time constant in the low frequencies region, which associates with the reactions for low-carbon steel corrosion caused by the corrosive medium penetrating into the cracks. A suitable equivalent circuit (shown in Fig. 7) was used to model the corrosion behavior. This equivalent circuit has been used for similar coating and Nyquist plots by other authors as well (Ref 23). In this equivalent circuit, R_s is the solution resistance, C_{coat} is the capacitance of the Ni-based alloy coating, including the pores in the outer layer of the coating, R_{pore} represents the resistance resulting from the formation of ionic conduction paths across the defect of coating, C_{dl} is the double-layer capacitance between the electrolyte and coating/substrate within the pores, and R_{ct} is the charge transfer resistance of the coating/substrate interface (Ref 23).

Fitted data using the equivalent electrical circuits are presented in Table 2. It is shown that R_{pore} values decrease with the increasing $Na_2MoO_4{\cdot}2H_2O$ content in the electroplating bath. As the result of morphological analysis, more rugged coatings were obtained and defects such as microcracks would be induced when the $Na_2MoO_4{\cdot}2H_2O$ content increases. These defects would offer paths for corrosive medium conduction and

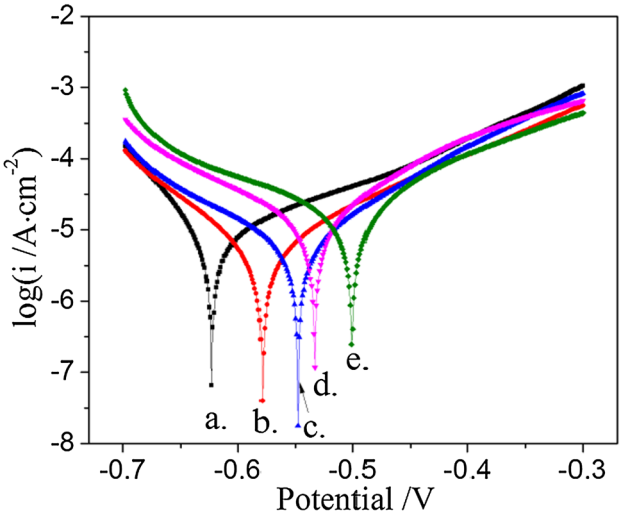

Fig. 5 Tafel polarization plots of Ni-Cu and Ni-Cu-Mo alloys electroplated in the bath containing different $Na_2MoO_4{\cdot}2H_2O$: (a) 0 g/L, (b) 20 g/L, (c) 40 g/L, (d) 60 g/L, (e) 80 g/L

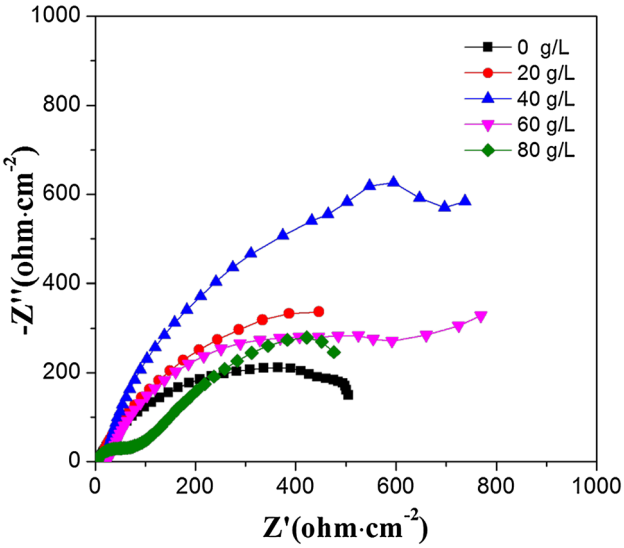

Fig. 6 Nyquist plots of Ni-Cu and Ni-Cu-Mo coatings electroplated in the bath containing different $Na_2MoO_4{\cdot}2H_2O$: (a) 0 g/L, (b) 20 g/L, (c) 40 g/L, (d) 60 g/L, (e) 80 g/L

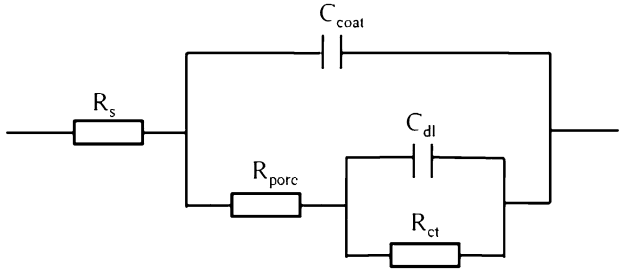

Fig. 7 Equivalent circuit for impedance measurements

Table 2 Corrosion data obtained from potentiodynamic polarization curves and EIS spectra using the equivalent circuit shown in Fig. 7

		Polarization		EIS		
Samples	**$Na_2MoO_4{\cdot}2H_2O$, g/L**	**E_{corr}, V**	**i_{corr}, μA/cm²**	**R_s, Ω cm²**	**R_{pore}, Ω cm²**	**R_{ct}, Ω cm²**
a	0	−6.22	4.21	7.4	329.4	422.2
b	20	−5.80	2.14	10.5	288.5	528.1
c	40	−5.48	1.91	17.5	258.0	1204.0
d	60	−5.32	4.90	23.7	154.8	541.0
e	80	−4.98	6.46	3.3	86.6	436.4

be adverse to its anti-corrosion properties. What is more, the Ni-Cu-Mo coating obtained in electroplating bath of 40 g/L $Na_2MoO_4{\cdot}2H_2O$ (shown in Table 2) has a highest R_{ct} value, confirming the most excellent corrosion resistance. There is a significant coherence between results obtained from potentiodynamic polarization and impedance techniques, where these two different techniques present the same trend of corrosion resistance.

4. Conclusions

In the present work, Ni-Cu-Mo ternary alloy coatings were electrodeposited on low-carbon steel substrates and their corrosion resistance has been investigated. Conclusions drawn from this work are listed as follows:

1. The surface of the electroplated Ni-Cu coating is homogeneous with fine grain, while Ni-Cu-Mo ternary alloy coating exhibits a rough, nodular morphology. The roughness of electroplated coating increases with the increasing of $Na_2MoO_4{\cdot}2H_2O$ in the bath.
2. The Ni-Cu-Mo coating is mainly composed of fcc-Ni phase and a small amount of NiCu phase. Increasing of $Na_2MoO_4{\cdot}2H_2O$ in the bath would decrease Cu and increase Mo contents of Ni-Cu-Mo coatings.
3. The coating prepared in bath containing 40 g/L $Na_2MoO_4{\cdot}2H_2O$ has the highest corrosion resistance in 3.5 wt.% NaCl solution, which as a result of Mo which has a beneficial effect on the corrosion behavior and reduces microcracking appeared on the surface.

Acknowledgment

This paper is financially supported by the Natural Science Foundation of China (51504104) and Natural Science Foundation of Jiangxi Province of China (20151BAB216012, 20161BAB206141).

References

1. D. Clark, D. Wood, and U. Erb, Industrial Applications of Electrodeposited Nanocrystals, *Nanostruct. Mater.*, 1997, **9**(1), p 755–758
2. S. Zhang, F. Cao, L. Chang et al., Electrodeposition of High Corrosion Resistance Cu/Ni-P Coating on AZ91D Magnesium Alloy, *Appl. Surf. Sci.*, 2011, **257**(21), p 9213–9220
3. Y. Wang, Q. Zhou, K. Li et al., Preparation of Ni-W-SiO_2 Nanocomposite Coating and Evaluation of Its Hardness and Corrosion Resistance, *Ceram. Int.*, 2015, **41**(1), p 79–84
4. M. Alper, H. Kockar, M. Safak et al., Comparison of Ni-Cu Alloy Films Electrodeposited at Low and High pH Levels, *J. Alloy. Compd.*, 2008, **453**(1), p 15–19
5. S.K. Ghosh, G.K. Dey, R.O. Dusane et al., Improved Pitting Corrosion Behaviour of Electrodeposited Nanocrystalline Ni-Cu Alloys in 3.0 wt.% NaCl Solution, *J. Alloy. Compd.*, 2006, **426**(1), p 235–243
6. U. Sarac, R.M. Öksüzoğlu, and M.C. Baykul, Deposition Potential Dependence of Composition, Microstructure, and Surface Morphology of Electrodeposited Ni-Cu Alloy Films, *J. Mater. Sci.: Mater. Electron.*, 2012, **23**(12), p 2110–2116
7. M. Haciismailoglu and M. Alper, Effect of Electrolyte pH and Cu Concentration on Microstructure of Electrodeposited Ni-Cu Alloy Films, *Surf. Coat. Technol.*, 2011, **206**(6), p 1430–1438
8. Q. Zhou, J. Jiang, Q. Zhong et al., Preparation of Cu-Ni-Fe Alloy Coating and Its Evaluation on Corrosion Behavior in 3.5% NaCl Solution, *J. Alloy. Compd.*, 2013, **563**, p 171–175
9. U. Sarac and M.C. Baykul, Microstructural and Morphological Characterizations of Nanocrystalline Ni-Cu-Fe Thin Films Electrodeposited from Electrolytes with Different Fe Ion Concentrations, *J. Mater. Sci. Mater. Electron.*, 2014, **25**(6), p 2554–2560
10. K.L. Lin, Y.L. Chang, C.C. Huang et al., Microstructure Evolution of Electroless Ni-P and Ni-Cu-P Deposits on Cu in the Presence of Additives, *Appl. Surf. Sci.*, 2001, **181**(1), p 166–172
11. Q. Yu, Z. Zeng, W. Zhao et al., Fabrication of Adhesive Superhydrophobic Ni-Cu-P Alloy Coatings with High Mechanical Strength by One Step Electrodeposition, *Colloids Surf., A*, 2013, **427**, p 1–6
12. A. Xia, C. Jin, D. Du et al., Effects of Impurity Na+ Ions on the Structural and Magnetic Properties of Ni-Zn-Cu Ferrite Powders: An Improvement for Chemical Coprecipitation Method, *J. Magn. Magn. Mater.*, 2011, **323**(15), p 2080–2082
13. E. Beltowska-Lehman, Electrodeposition of Protective Ni-Cu-Mo Coatings from Complex Citrate Solutions, *Surf. Coat. Technol.*, 2002, **151**, p 440–443
14. E. Beltowska-Lehman and E. Chassaing, Electrochemical Investigation of the Ni-Cu-Mo Electrodeposition System, *J. Appl. Electrochem.*, 1997, **27**(5), p 568–572
15. E. Beltowska-Lehman and P. Ozga, Effect of Complex Formation on the Diffusion Coefficient of Cu II, in Citrate Solution Containing Ni II, and Mo VI, *Electrochim. Acta*, 1998, **43**(5), p 617–629
16. E. Beltowska-Lehman, A. Bigos, P. Indyka et al., Electrodeposition and Characterisation of Nanocrystalline Ni-Mo Coatings, *Surf. Coat. Technol.*, 2012, **211**, p 67–71
17. R. Abdel-Karim, J. Halim, S. El-Raghy et al., Surface Morphology and Electrochemical Characterization of Electrodeposited Ni-Mo Nanocomposites as Cathodes for Hydrogen Evolution, *J. Alloys Compd.*, 2012, **530**, p 85–90
18. E. Beltowska-Lehman and P. Indyka, Kinetics of Ni-Mo Electrodeposition from Ni-Rich Citrate Baths, *Thin Solid Films*, 2012, **520**(6), p 2046–2051
19. H. Alimadadi, M. Ahmadi, M. Aliofkhazraei et al., Corrosion Properties of Electrodeposited Nanocrystalline and Amorphous Patterned Ni-W Alloy, *Mater. Des.*, 2009, **30**(4), p 1356–1361
20. E.J. Podlaha and D. Landolt, Induced Codeposition I. An Experimental Investigation of Ni-Mo Alloys, *J. Electrochem. Soc.*, 1996, **143**(3), p 885–892
21. L.S. Sanches, S.H. Domingues, C.E.B. Marino et al., Characterisation of Electrochemically Deposited Ni-Mo Alloy Coatings, *Electrochem. Commun.*, 2004, **6**(6), p 543–548
22. Q. Zhou, Y. Wang, H. Wu et al., Preparation of Passive Cu-Ni-Fe Coating on Low-Carbon Steel for Improving Corrosion Resistance, *Surf. Coat. Technol.*, 2012, **207**, p 503–507
23. K.R. Sriraman, S.G.S. Raman, and S.K. Seshadri, Corrosion Behaviour of Electrodeposited Nanocrystalline Ni-W and Ni-Fe-W Alloys, *Mater. Sci. Eng. A*, 2007, **460**, p 39–45